Reconstruction of the neutrino mass as a function of redshift

Christiane S. Lorenz[1,*] Lena Funcke[2,†] Matthias Löffler[3] and Erminia Calabrese[4]

[1]*Institute for Particle Physics and Astrophysics, ETH Zurich, Wolfgang-Pauli-Strasse 27,*
CH-8093 Zurich, Switzerland
[2]*Perimeter Institute for Theoretical Physics, 31 Caroline Street North,*
Waterloo, Ontario N2L 2Y5, Canada
[3]*Seminar for Statistics, Department of Mathematics, ETH Zurich, Raemistrasse 101, CH-8092 Zurich,*
Switzerland
[4]*School of Physics and Astronomy, Cardiff University, The Parade, Cardiff CF24 3AA, United Kingdom*

We reconstruct the neutrino mass as a function of redshift, z, from current cosmological data using both standard binned priors and linear spline priors with variable knots. Using cosmic microwave background temperature, polarization and lensing data, in combination with distance measurements from baryonic acoustic oscillations and supernovae, we find that the neutrino mass is consistent with $\sum m_\nu(z) = $ const. We obtain a larger bound on the neutrino mass at low redshifts coinciding with the onset of dark energy domination, $\sum m_\nu(z = 0) < 1.46$ eV (95% CL). This result can be explained either by the well-known degeneracy between $\sum m_\nu$ and Ω_Λ at low redshifts, or by models in which neutrino masses are generated very late in the Universe. We finally convert our results into cosmological limits for models with nonrelativistic neutrino decay and find $\sum m_\nu < 0.21$ eV (95% CL), which would be out of reach for the KATRIN experiment.

I. INTRODUCTION

Cosmological surveys and particle physics experiments are independent and complementary probes of neutrino properties. Neutrino oscillation experiments have measured the squared mass differences between neutrino mass eigenstates, giving a lower bound of 59 meV for the total sum of the neutrino masses, $\sum m_\nu$ [1]. In addition, the Karlsruhe Tritium Neutrino Experiment (KATRIN) has constrained the electron neutrino mass to be lower than $m_{\nu,e} < 0.8$ eV at 90% CL [2,3]. Independent from these constraints, measurements of the cosmic microwave background (CMB) with the *Planck* satellite mission, combined with distance measurements from baryonic acoustic oscillations (BAO) from the Sloan Digital Sky Survey (SDSS) and 6dF have provided a tight upper bound on the total sum of neutrino masses, $\sum m_\nu < 120$ meV at 95% CL [4].

Contrary to neutrino mass direct detection limits, the cosmological neutrino mass bound assumes a specific cosmological model, usually the ΛCold Dark Matter (ΛCDM) model or its single-parameter extensions. In more extended cosmological models, the cosmological neutrino mass limits can become less stringent due to opening wider parameter spaces and/or covering more complex physics scenarios.

On the one hand, the *lower* bound of $\sum m_\nu = 59$ meV imposed by neutrino oscillation experiments can be relaxed in cosmological analyses to $\sum m_\nu = 0$ meV, for example, if cosmological neutrinos disappear in the late Universe. Although the original "neutrinoless Universe" proposal [5] has been ruled out,[1] other scenarios like models predicting postrecombination neutrino mass generation and subsequent relic neutrino annihilation [9] are still possible. In such models, the neutrino mass parameter cannot be captured using cosmological data and can only be measured using terrestrial and astrophysical experiments such as KATRIN. The possible cosmological disappearance of the neutrino mass parameter has also been proposed in the context of modified gravity theories [10–12]; these should soon be tested with surveys like Euclid [12]. If we allow for strong fine tuning, another possibility to eliminate the cosmological neutrino mass bounds would be to postulate a new light scalar particle that couples to neutrinos, with a coupling constant that needs to be smaller than $g \sim 10^{-7}$ to avoid laboratory constraints [13].

On the other hand, the *upper* cosmological neutrino mass bound is sensitive to a number of model assumptions and can be slightly relaxed, for example when the dark energy

---

*chrlorenz@phys.ethz.ch
†lfuncke@perimeterinstitute.ca

[1]By free-streaming of the cosmic neutrino background before photon decoupling [6,7], by the resulting phase shift in the CMB peaks [8], and by precise CMB measurements of the effective number of species in the early Universe [4].

equation of state is allowed to vary in time [14–21], when the curvature of the Universe is not fixed [21], when considering additional relativistic degrees of freedom [4], or when assuming non-standard momentum distributions of the cosmic neutrinos [22]. Moreover, it has been shown that the cosmological neutrino mass bound can be substantially weakened when neutrinos are unstable and thus their lifetime is smaller than the age of the Universe [23–27] or when neutrino masses are varying in time [9,28–30]. Note, however, that the strongly relaxed neutrino mass bounds of $\sum m_\nu < 0.9$ eV (95% CL) with neutrino decays [24] or $\sum m_\nu < 4.8$ eV (95% CL) with time-varying neutrino masses [30] have been derived from previous releases of cosmological data, including the *Planck* 2015 CMB data. The neutrino mass bound has been substantially tightened with the *Planck* 2018 release, $\sum m_\nu = 0.12$ eV (95% CL, *Planck* 2018 TTTEEE + lowE + lensing + BAO [4]) and therefore, we expect the above-mentioned bounds also to change.

In a previous publication [30], some of us investigated how the standard cosmological neutrino mass bound would be affected if neutrino masses were to be generated late in the Universe. This analysis suggested that the combination of current CMB temperature, polarization and lensing data, as well as BAO and supernovae (SN) data prefers neutrino masses to be generated at low redshifts, allowing a significantly larger cosmological neutrino mass upper bound. An alternative interpretation of the results is that current cosmological datasets do not necessarily require neutrinos to be massive, pushing the scale factor of the phase transition in the model to very low redshifts. The trend of larger neutrino mass bounds in the late Universe had already been noted before (see, e.g., Refs. [29,31–36] and references therein). This could either arise due to the well-known degeneracy between neutrino masses and dark energy, or be explained by new physics beyond the Standard Model of cosmology. In particular, it seems striking that the energy scales of dark energy and neutrino masses are numerically very close, $\sqrt[4]{\rho_\Lambda} \sim m_\nu \sim$ meV. If cosmological data permit larger neutrino masses during dark energy domination, there could be an intriguing theoretical connection between these two phenomena (see, e.g., Refs. [9,28,37–40] and references therein).

The tight neutrino mass limit from cosmology is making a direct detection from Tritium β-decay experiments like KATRIN very challenging. Indeed, KATRIN's target sensitivity of 200 meV at 90% CL for the ν_e mass [41] will unlikely hit the cosmological limit obtained in either ΛCDM or its simple extensions [4,21]. Assuming all observations and analysis assumptions are correct and free of systematic effects, we are entering a regime where a direct detection of neutrino masses with particle detectors such as KATRIN could become a strong hint for non-standard neutrino physics. At the same time, the next generation of cosmological surveys aim to improve their

reach in neutrino mass sensitivity and to make the first detection [42,43].

To work toward these future goals, we present here a model-independent approach to investigate the possibility that neutrino masses change on cosmological timescales, reconstructing the neutrino mass as a function of redshift.

A similar methodology has been applied to reconstruct possible variations in other cosmological parameters, in particular dark energy parameters [36,44–56] and the Hubble parameter [36,57–62] as a function of redshift, the shape of the primordial power spectrum as a function of wave number [63–67], and parameters describing deviations from general relativity as a function of redshift and wave number [68]. Exploring variations of cosmological parameters in time also gains in importance in light of tensions between parameters inferred from current high- and low-redshift data (see, e.g., Ref. [69]).

In general, reconstructions fully accounting for degeneracies and the interplay between cosmological parameters, such as the dark matter density and dark energy parameters, are especially hard to achieve [70–72]. In the case of the neutrino mass, a model-independent reconstruction is particularly challenging. A comprehensive model for time-varying neutrino masses would require an interaction with other energy sectors, such as dark radiation or dark energy, to satisfy energy conservation laws. Additionally, including such interactions permits to fully capture and exploit the physics signatures of the model. While in the case of dark radiation this interaction is negligible for many cosmological scenarios (e.g., the dark radiation resulting from neutrino decays has negligible cosmological impact [24]), in the case of dark energy this interaction could alter $w_{\mathrm{de}}(z)$ and thus generate multiple signatures that allow us to place stronger limits on the model.

In this paper, we take a conservative approach and use a generic function to model the neutrino mass sum. We also ignore potential additional constraining power coming from the inclusion of the coupling between the neutrino and the dark sector which is theory specific, and perform a model-independent analysis that only focuses on neutrinos without assuming any specific interactions with other dark sectors. This yields a conservative approach in the modelling but not necessarily the most conservative neutrino mass constraints (see the discussion in Sec. V). The method used here expands on the work done in Ref. [30], which assumed a specific time-varying neutrino mass model, and also spans models with neutrino decays for which we will set new limits.

The paper is structured as follows. In Sec. II we explain the theoretical background of cosmological neutrino mass constraints and neutrino mass models. In Sec. III we present our methodology, in particular the different datasets and reconstruction methods. We present our results in Sec. IV and summarize and discuss them in Sec. V.

II. THEORETICAL BACKGROUND

A. Neutrino mass constraints from cosmological probes

At the beginning of their cosmic journey, neutrinos are relativistic particles and behave as a radiation component in the early Universe. When their kinetic energy term drops below the mass term due to cooling in an expanding Universe, neutrinos start to behave as nonrelativistic, massive particles. The redshift of this transition is inversely proportional to the neutrino mass [73]: neutrinos with a smaller mass become nonrelativistic at a later time compared to neutrinos with a higher mass. Neutrino masses thus affect cosmological observations during different cosmic epochs, which in turn allows us to probe $\sum m_\nu$ at different redshifts.

1. The cosmic microwave background

Constraining neutrino properties with the CMB has been a rich research area with extensive literature (see, e.g., Refs. [74–76]). To summarize, the key effects we look for in CMB probes are:

(i) Effects on the background evolution of the Universe via changes in the angular diameter distance at recombination, $D_A(z_{\rm rec})$ and the Hubble parameter [74,75]. In general, there is a strong degeneracy between neutrino parameters and the Hubble constant [74,77–80].

(ii) Effects on the evolution of perturbations. In particular, the integrated Sachs-Wolfe effect is affected, both at early times during radiation domination (eISW) [74,75], as well at late times when dark energy starts to dominate the evolution of the Universe (ℓISW) [81]. The eISW depends on the relativistic degrees of freedom, $N_{\rm eff}$, as well on neutrino masses, but in a different way. Whereas $N_{\rm eff}$ mostly changes the amplitude of the first peak in the CMB anisotropy power spectrum, neutrino masses affect the amplitude of the eISW on a large range of multipoles depending on the neutrino mass and the corresponding free-streaming scale [74,75,82]. The ℓISW effect dominates at $\ell < 30$ and is therefore elusive because of cosmic variance in CMB data alone. However, when cross-correlated with galaxy number counts, this effect is a promising avenue for measuring neutrino masses [83].

(iii) Effects on the matter distribution deflecting the CMB photons by gravitational lensing [84]. This will leave both an imprint on the CMB temperature and polarization anisotropies (in the high-ℓ region of the spectra), as well as generate a CMB lensing convergence signal, $C_\ell^{\phi\phi}$. The latter probe will capture the small-scale suppression of the matter power spectrum due to large neutrino thermal velocities and corresponding free-streaming out of density fluctuations [75,85]. Depending on whether the neutrino wavelength is above or below the free-streaming wavelength, neutrinos cluster as cold dark matter and baryons, or free-stream out of gravitational wells. This slows down the clustering of matter, leading to a suppression of the matter power spectrum on the corresponding scales which is more pronounced for larger neutrino masses [86]. The CMB damping tail is measured with high precision with current data [87–89] and CMB lensing is now in a high signal-to-noise regime [90,91].

(iv) The optical depth to reionization τ is degenerate with the amplitude of scalar primordial fluctuations A_s. Since the amount of clustering of cosmic structures is tightly linked to $\sum m_\nu$, this in turn becomes a strong degeneracy between τ and $\sum m_\nu$. CMB polarization measurements of τ enable us to obtain a tighter constraint on $\sum m_\nu$ [16,92].

2. Baryonic acoustic oscillations

Before CMB decoupling, baryons and photons are tightly coupled to each other. At the time of recombination, the CMB photons decouple from the baryons, and the oscillations of the baryon-photon fluid are frozen in the CMB anisotropies. In addition to the CMB, these oscillations also leave a characteristic imprint in the large scale structure of the Universe, both transverse as well as along the line of sight [93,94]. In particular, the size of the BAO is known, and therefore BAO can be used as standard rulers to infer either $H(z)r_s(z^*)$ or $D_A/r_s(z^*)$, where $D_A(z)$ is the angular diameter distance (see, e.g., Refs. [95,96] for reviews) and r_s the sound horizon at decoupling z^*. These quantities are in particular sensitive to the matter density $\Omega_m h^2$. BAO measurements allow to constrain the energy contribution of massive neutrinos to the matter density. The BAO feature has been detected in the clustering of galaxies [93,94,97], as well as in the clustering of low-redshift quasars [98–100], and in the correlations of Lyman-α systems [101,102] (see below). This latter probe provides an additional measurement to standard BAO data and extends BAO observations toward high redshifts.

3. Lyman-α forest

The absorption lines of neutral hydrogen in the intergalactic medium (IGM) in quasar spectra are sensitive to cosmological parameters, and probe cosmic structure formation at redshifts between $z \sim 2$–6. In particular, Lyman-α forest measurements characterize small structures on the scale of sub-Mpc to Mpc. This anchors the level of the matter power spectrum on scales between $k \sim 0.1$–2 and therefore probes the regime where the suppression of the matter power spectrum due to massive neutrinos is the most pronounced (see, e.g., Refs. [103–107]). The relevant summary statistic is the 1D flux power spectrum, which is related to the matter power spectrum using a nonlinear transformation [108,109]. The level of the 1D flux power

spectrum depends both on the amplitude of the linear matter power spectrum and on the sum of neutrino masses, resulting in a degeneracy between these two parameters [110]. This limits the ability of current Lyman-α forest measurements to constrain neutrino masses. The current upper bound from Lyman-α measurements alone is $\Sigma m_\nu <$ 0.71 eV (95% CL) [107]. Probing cosmological parameters with the Lyman-alpha forest is also challenging because of observational and astrophysical systematics, which need to be modeled in the analyses [111,112].

4. Supernovae

Measurements of the luminosity distance $D_L(z)$ from supernovae explosions are not directly sensitive to neutrino properties. However, they can be used to constrain dark energy parameters, such as the dark energy density Ω_Λ and the dark energy equation of state $w_{de}(z)$ (see, e.g., Ref. [113] for a review), which helps significantly to break degeneracies with neutrino parameters.

Combining the different cosmological probes described above enhances significantly the constraining power coming from only one of the datasets (see, e.g., Refs. [4,42,74,76,114]). This is due to the fact that (i) different probes are capturing the physics of the Universe at different redshifts, and (ii) different probes depend on different parameter combinations, which follow different degeneracy directions. For example, Ref. [74] describes in detail how the combination of CMB and BAO helps to break the $H_0 - \sum m_\nu$ degeneracy.

B. Neutrino mass models

Most of the possible neutrino mass models, in particular the ones arising from the famous seesaw mechanism [115–120], cannot be tested using cosmological data. From a cosmological perspective, more focus is then naturally placed on studying neutrino mass mechanisms that make cosmologically testable predictions, such as models providing neutrino mass variations on cosmologically interesting timescales.

As mentioned earlier, when allowing for the neutrino mass to vary as a function of redshift, an interaction with the dark energy or dark radiation sector is required to satisfy energy conservation laws. The most popular models that couple the neutrino and dark energy sectors are mass varying neutrino (MaVaN) scenarios (see, e.g., Ref. [28]). Here, the neutrinos couple to a light scalar field, which slowly rolls in a flat potential. Originally, this direct link between neutrino masses and dark energy was proposed to explain the similarity between the energy scales of neutrino masses and quintessence-like dark energy ($E \sim 10^{-3}$ eV). However, the coupling to a light scalar mediates an attractive force between the neutrinos and leads to bound state formation [121], such that the light scalar field can only explain dark energy under rather special circumstances (see, e.g., Refs. [37–39]). For example, the growing

neutrino quintessence model studied in Ref. [38] yields time-dependent neutrino masses, which vanish in the early Universe and raise from $m_\nu = 0$ eV at $a \lesssim 0.2$ to $m_\nu \sim$ 0.7 eV at $a = 1$.

Coupling the mass-varying neutrino sector to dark radiation is less trivial and usually occurs with simultaneously coupling both sectors to the dark energy sector. For example, it has been proposed that a simultaneous variation of neutrino masses, a light sterile neutrino fraction, and dark energy can be used to test certain aspects of the weak gravity conjecture [40].

Another gravitational avenue to couple neutrinos to dark energy and dark radiation is the gravitational neutrino mass model proposed in Ref. [9], which served as a motivation for the previous cosmological study in Ref. [30]. The key cosmological prediction of this model is that the cosmological neutrino mass parameter vanishes. Indeed, the model predicts massless neutrinos in the early Universe and the generation of neutrino masses in a late-time cosmological phase transition at $T \lesssim m_\nu$. In the phase transition, neutrino masses are generated, followed by neutrino decay into the lightest mass eigenstate and rapid annihilation into massless Goldstone bosons (see Refs. [9,122,123] for more details). Thus, the model predicts massless neutrinos in the early Universe and massless dark radiation in the late Universe. The intermediate regime with massive neutrinos, which exists directly after the phase transition, exists only for cosmologically negligible timescales. This implies that the cosmological neutrino mass parameter would be zero, as currently preferred by cosmological data [4]. This also implies that experiments aiming at a direct detection of the relic neutrino background, such as the proposed PTOLEMY experiment [124], would not be able to detect this background,[2] unless we allow for substantial neutrino asymmetries (see below).

If the model in Ref. [9] is extended by allowing for neutrino asymmetries (i.e., more neutrinos than antineutrinos or vice versa), not all neutrinos would find an antineutrino partner to annihilate, leaving behind a fraction of relic neutrinos with a nonzero cosmological mass parameter. As Ref. [30] demonstrated, even in this case, the cosmological neutrino mass bound would be substantially weakened to $\sum m_\nu < 4.8$ eV (95% CL). However, we note that this weakened bound was obtained with *Planck* 2015 data and is expected to become more stringent when including the *Planck* 2018 dataset. This is because the ΛCDM constraint on $\sum m_\nu$ strengthened by a factor of

---

[2]At first sight, one might expect that PTOLEMY could detect the massless Goldstone bosons, which are neutrino-composite bosons (similar to the light quark-composite mesons in QCD). However, the boson's energy is $E = T_\nu < m_\nu$, while the neutrino capture would release the other neutrino of the bound state, requiring an energy of at least m_ν. This would violate energy conservation, unless one of the neutrinos is almost massless. We thank Pedro Machado for bringing up this argument.

$\mathcal{O}(2)$ from $\sum m_\nu = 0.21$ eV (95% CL, *Planck* 2015 without polarization [125]) to $\sum m_\nu = 0.12$ eV (95% CL, *Planck* 2018 [4]).

Finally, neutrinos can couple to the dark radiation sector if they are unstable, with lifetimes shorter than the age of the Universe. In particular, 2-body decays of neutrinos into BSM particle species, such as massless or very light sterile neutrinos and Goldstone bosons, have been proposed to relax cosmological neutrino mass bounds. Early cosmological studies based on *Planck* 2015 data implied a relaxation of the cosmological neutrino mass bound up to $\sum m_\nu \lesssim 0.9$ eV [24–26]. As above, this bound is expected to become tighter when including *Planck* 2018 data (see Sec. IV C). Thus, neutrino decay can only slightly alleviate cosmological bounds, similar to other extensions of the ΛCDM model, such as dynamical dark energy. However, such models leave the intriguing possibility of observing less (or even completely vanishing) neutrino mass in the late Universe, similar to the model proposed in Ref. [9], and thus make cosmological observations crucial for determining the neutrino mass origin and beyond-SM neutrino interactions.

These and other theoretical motivations to study neutrino mass variations on cosmologically interesting timescales, which typically yield nontrivial interactions with other cosmological sectors such as dark energy and dark radiation, are the main rationale for the work that we present here.

III. METHODOLOGY

A. Data

Motivated by the expected contribution highlighted in Sec. II A, we include the following datasets in our analysis:

(1) CMB and CMB lensing: We use CMB temperature, polarization and lensing data from the *Planck* 2018 data release [4].

(2) BAO: We use BAO from 6dF [126], the Sloan Digital Sky Survey (SDSS) DR7 Main Galaxy Sample (MGS) [127] and the SDSS Baryon Oscillation Spectroscopic Survey (BOSS) twelfth data release (DR12) [128]. The mild discrepancies seen between *Planck* and Lyman-alpha BAO data have decreased in recent releases of the Lyman-alpha BAO from SDSS DR14 eBOSS [129,130]. Therefore we include also this additional BAO dataset which provide two data points at $z \sim 1.5$ and $z \sim 2.3$. We also include the BAO measurement from quasars from the 14th data release of the extended BOSS (eBOSS) quasar sample [99], giving us another data point at $z \sim 1.5$.

(3) Supernovae: We additionally add type IA supernova data from from the Pantheon Supernovae Sample [131] in order to break the degeneracies between dark energy and neutrino masses.

We demonstrate the impact of these specific datasets later in Sec. IV, and summarize their respective redshift range in Table I.

B. Reconstruction method

We modify the publicly available Einstein-Boltzmann code CAMB [133] and the corresponding Monte-Carlo Markov chain package COSMOMC [134] in order to implement different reconstruction methods for redshift-dependent neutrino masses.

1. Binned reconstruction

As a first attempt, we parametrize the neutrino mass with a step function for which it is assumed that the neutrino mass has a constant positive amplitude in each redshift bin. In the statistics literature this is called a regressogram [135]. To maximally exploit our datasets we use a parametrization with six redshift intervals:

$$\sum m_\nu(z) = \begin{cases} \sum m_{\nu,0} & (0 \leq z < z_1) \\ \sum m_{\nu,1} & (z_1 \leq z < z_2) \\ \sum m_{\nu,2} & (z_2 \leq z < z_3) \\ \sum m_{\nu,3} & (z_3 \leq z < z_4) \\ \sum m_{\nu,4} & (z_4 \leq z < z_5) \\ \sum m_{\nu,5} & (z \geq z_5). \end{cases} \quad (1)$$

TABLE I. List of datasets used in the analyses performed in this work and their corresponding redshift range.

Dataset	Redshift range
Planck 2018 CMB TTTEEE [4,88]	Mostly $z = 1100$
Planck 2018 CMB lowl [4,88]	Mostly $z = 1100$
Planck 2018 CMB lowE [4,88]	Mostly $z = 8$ and $z = 1100$
Planck 2018 CMB lensing [4,132]	$0 \leq z \leq 1100$
BAO (6dF) [126]	$z = 0.106$
BAO (SDSS DR7 BOSS MGS) [127]	$z = 0.15$
BAO (SDSS DR12 BOSS) [128]	$z = 0.38, 0.51, 0.61$
BAO (SDSS DR14 eBOSS quasars)[99]	$z = 1.52$
BAO (SDSS DR14 eBOSS Ly-α) [129]	$z = 2.34$
BAO (SDSS DR14 eBOSS cross Ly-α-QSO) [129]	$z = 2.35$
SN (Pantheon) [131]	$0.01 < z < 2.3$

We choose the edges of the redshift bins to pinpoint specific transitions in the composition of the Universe and to highlight the impact of using different cosmological probes. We set $z_1 = 0.5$, $z_2 = 3$, $z_3 = 10$, $z_4 = 100$ and $z_5 = 1100$. The first bin explores $\sum m_\nu$ during dark energy domination, the second bin spans the BAO interval, the third bin includes most of the remaining information expected in CMB lensing [136], the fourth bin covers intermediate redshifts, and the second to the last bin stretches out to the time of CMB decoupling. The last bin for $z > 1100$ captures all the integrated information of the pre-recombination Universe. This choice of bins will also allow us to set constraints on neutrino decay models [23–26], as described in Sec. IV C. The neutrino masses in the individual bins are five additional parameters in the model, compared to the standard ΛCDM model with massive neutrinos. The discontinuity in the binned $\sum m_\nu(z)$ leads only to small discontinuities in related quantities, such as the Hubble rate $H(z)$, which however cause no numerical instabilities in the analysis. A similar parametrization has recently been used for the reconstruction of the dark energy equation of state $w_{\rm de}(z)$ from gamma-ray bursts [137].

2. Spline priors

To perform a smoother fit and to potentially identify features in the neutrino mass sum that are hidden in the binned reconstruction, we also consider Bayesian regression splines with variable knot points [138].

The knots correspond to the bin margins of the regressogram prior function described above, and model change points where the trajectory of the neutrino mass might change its slope. Previous literature in cosmology has often used splines with fixed knot positions (see, e.g., [36,59,64]). This, however, requires to choose the positions of the knots in advance and can therefore significantly influence or bias the result of the reconstruction. Here, we estimate the position of the knots from the data and include them as free parameters in the analysis. Using variable knot positions yields a more flexible fit than in the case with fixed knots and allows the fit to adapt to underlying features of the model. This methodology has previously successfully been applied several times in cosmology [48,139,140], most recently in Ref. [62].

Compared to binned priors, the resulting reconstruction is smooth and not piecewise constant anymore. We model two knots, z_1 and z_2, and linearly interpolate between $\sum m_{\nu,z_0}$, $\sum m_{\nu,z_1}$, $\sum m_{\nu,z_2}$ and $\sum m_{\nu,z_3}$. For our analysis, we choose $z_0 = 0$ and $z_3 = 1100$. In that case, the neutrino mass at redshift z is given by

$$\sum m_\nu(z)$$
$$= \begin{cases} \sum m_{\nu,z_0} + \left(\sum m_{\nu,z_1} - \sum m_{\nu,z_0}\right)\frac{z}{z_1} & (z_0 \leq z < z_1) \\ \sum m_{\nu,z_1} + \left(\sum m_{\nu,z_2} - \sum m_{\nu,z_1}\right)\frac{z-z_1}{z_2-z_1} & (z_1 \leq z < z_2) \\ \sum m_{\nu,z_2} + \left(\sum m_{\nu,z_3} - \sum m_{\nu,z_2}\right)\frac{z-z_2}{z_3-z_2} & (z_2 \leq z < z_3) \\ \sum m_{\nu,z_3} & (z \geq z_3). \end{cases}$$
$$(2)$$

We then choose a uniform prior on the logarithm of the corresponding redshift with $-1 \leq \log_{10}(z_i)_{i=1,2} \leq 3.041$, covering the entire redshift region until recombination and focusing on low redshifts where most of the data is located. We further need to impose that z_2 has to be equal or larger than z_1, in accordance to the definition above in Eq. (2). In addition, we choose $z_{1,2} > 0.1$, corresponding to the lowest redshift of the BAO dataset (see Table I).

With this parametrization, we have five additional free parameters compared to the standard ΛCDM with massive neutrinos, three for $\sum m_\nu$ at z_1, z_2 and z_3, and two for the positions of z_1 and z_2. In order to obtain pointwise credible bands for $\sum m_\nu(z)$, we compute the neutrino mass sum for two hundred points in z as derived parameters with `GetDist` [141] to sample well the entire redshift range. We then compute pointwise the mean and credible intervals for each point in z.

IV. CONSTRAINTS FROM CURRENT DATA

For our neutrino mass reconstruction, we run MCMC chains with our modified version of COSMOMC. Since both our methods only touch the neutrino mass modeling, we vary the standard ΛCDM parameters alongside with the new parameters of the reconstruction: the cold dark matter density $\Omega_c h^2$, the baryon density $\Omega_b h^2$, the scalar spectral index n_s, the amplitude of primordial fluctuations A_s and the optical depth to reionization τ. In addition, we have six additional parameters for the reconstruction with fixed bins ($\sum m_{\nu,0}$, $\sum m_{\nu,1}$, $\sum m_{\nu,2}$, $\sum m_{\nu,3}$, $\sum m_{\nu,4}$ and $\sum m_{\nu,5}$), and six for the reconstruction with linear splines and variable knots [$\sum m_{\nu,z_0}$, $\sum m_{\nu,z_1}$, $\sum m_{\nu,z_2}$, $\sum m_{\nu,z_3}$ and the position of the knots $\log_{10}(z_1)$ and $\log_{10}(z_2)$]. We choose a uniform prior between [0:5] for $\sum m_\nu$ in the individual redshift bins (similarly to the *Planck* 2018 analysis [4]), and we do not assume a specific correlation between the values of $\sum m_\nu$ in the different bins, leaving them to vary independently. In addition, we assume a normal neutrino mass hierarchy in line with current cosmological constraints [4,21,142]. The choice of the mass hierarchy should not significantly affect our final results presented in Sec. IV, as current cosmological data

cannot (yet) distinguish between the different neutrino mass hierarchies [21,76,142–151].

A. Binned reconstruction

We show the results of the binned neutrino mass reconstruction in Fig. 1, and in Table II. We plot both the 95% and the 68% CL upper limits for each mass parameter, as well as the 95% limit for $\sum m_\nu(z) = $ const. (i.e., the standard single parameter extension of ΛCDM for massive neutrinos) obtained from the same data combinations. We always plot the 95% CL and 68% CL one-tail upper limits, e.g., we have removed the 32% and 5% highest samples for these limits. For consistency we choose the same type of limits for all the individual redshift bins, and can therefore compare better the results for the individual bins and data combinations. For the full data combination including CMB, CMB lensing, BAO and SN, we find

$$\sum m_\nu(0 \leq z < 0.5) < 1.13 \text{ eV}$$
$$\sum m_\nu(0.5 \leq z < 3) < 0.42 \text{ eV}$$
$$\sum m_\nu(3 \leq z < 10) < 0.37 \text{ eV}$$
$$\sum m_\nu(10 \leq z < 100) < 0.19 \text{ eV}$$
$$\sum m_\nu(100 \leq z < 1100) < 0.32 \text{ eV}$$
$$\sum m_\nu(z \geq 1100) < 0.40 \text{ eV} \quad (95\% \text{ CL}).$$

These results are consistent with neutrino masses constant in time. In addition, we observe that the neutrino mass bound becomes less stringent at low redshifts ($z \leq 3$), and at very high redshifts ($z \geq 1100$). The large neutrino mass bound at low redshifts could arise due to the well-known degeneracy between the neutrino mass sum and the dark energy density (see below). It could also point at a very late generation of neutrino masses in the Universe, and would therefore be consistent with the trend seen in Ref. [30]. In the Standard Model of cosmology, the neutrino masses are generated during the electroweak or earlier phase transitions.

Our plots also allow us to note the contribution to the constraint from different probes.

1. Top row

In the top row of Fig. 1, we plot the z-dependent constraints on the neutrino mass sum from CMB anisotropy data alone. Because the binned reconstruction introduces more free parameters, the constraints in all bins are consistent but systematically larger than the standard neutrino mass bound from the latest *Planck* release [1,4].[3] The CMB anisotropy data put a strong constraint on $\sum m_\nu$ at high redshifts, but only a weak constraint at low

---

[3]Note that the $\sum m_\nu(z) = $ const. line should be compared to the 95% shaded region.

redshifts. We also note that the neutrino mass sum in the lowest redshift bin is unconstrained. In this bin the CMB data alone provides insufficient constraining power. As described earlier, at low redshifts, the CMB anisotropy data would mostly be sensitive to neutrino masses via the late integrated Sachs-Wolfe effect at low multipoles ℓ, which is cosmic variance limited and subject to significant parameter degeneracies. In the lowest redshift bin ($0 < z < 0.5$), the CMB has only little constraining power, and the prior (with prior mean $\sum m_\nu = 2.5$ eV) dominates the result of the reconstruction. At intermediate redshifts, the data strongly constrain the neutrino mass through the lensing of the CMB anisotropies which will be picked up here as a smoothing of the temperature and polarization data, and the impact of neutrinos on the background evolution (see the discussion in Sec. II). At high redshifts close to recombination, we observe a small increase in the uncertainty of $\sum m_\nu$. This might be due to the fact that at recombination the constraint on $\sum m_\nu$ comes mostly from the early integrated Sachs-Wolfe effect, the CMB damping tail, and background effects, while all other effects from neutrino masses only become relevant at intermediate to low redshifts.

2. Second row

In the second row in Fig. 1, we plot the constraints on $\sum m_\nu(z)$ from CMB anisotropies plus the CMB lensing reconstruction. The CMB lensing kernel peaks around $z \sim 2$ (see, e.g., Refs. [152,153]) and carries constraining power on the bin between $0.5 \leq z < 3$. Other constraints are also improved by an indirect effect: CMB lensing is also sensitive to the total matter density and the dark energy density [154], and therefore helps to constrain $\sum m_\nu(0 < z < 0.5)$ by partially breaking the tridimensional degeneracy between Ω_Λ, Ω_m, and $\sum m_\nu$. This can also be seen in Fig. 2, where we show the results for $\sum m_\nu$ in the different bins, as well as its correlation with Ω_Λ and Ω_m.

3. Third row

The BAO data points used in this work are distributed over the whole redshift range between $z = 0.1$–2.35. This mostly improves the constraints in the first two neutrino mass bins. In addition, the inclusion of BAO reduces significantly the degeneracy between Σm_ν and Ω_m, and therefore also improves the overall constraints in all redshift bins.

4. Bottom row

We include SN data from the Pantheon 18 data set to constrain further the dark energy component. We observe the smallest uncertainty of $\sum m_\nu$ in the bin between $10 \leq z \leq 100$. The sensitivity of the neutrino mass bound starts to weaken at a similar redshift as the onset of dark energy domination (see below). The degeneracy between
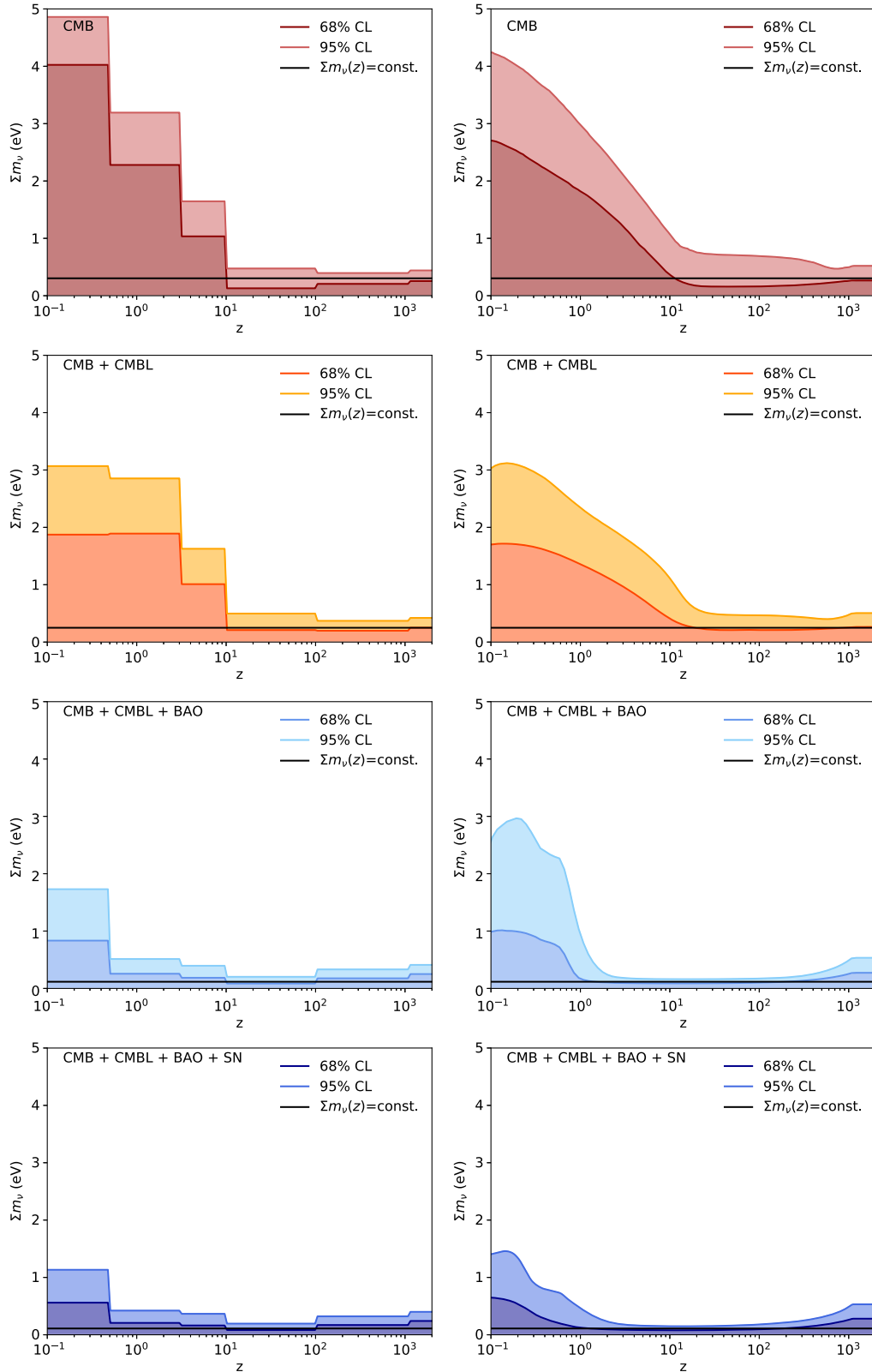
FIG. 1.   Reconstructed upper bounds of the neutrino mass as function of redshift. The panels from top to bottom show incremental addition of data starting from *Planck* 2018 CMB temperature and polarization, and then subsequently adding *Planck* CMB lensing, BAO from BOSS DR12, 6dF and MGS, eBOSS DR14 quasars and Lyman-alpha, and SN from Pantheon 18. The left panels show the results obtained with the binned parameterization and the right panels the limits from the reconstruction with linear splines and variable knots. In all cases, we also report with the black solid line the 95% CL constraint from the same data combination for $\sum m_\nu(z) = $ const. (i.e., the standard single parameter extension of ΛCDM for massive neutrinos).

TABLE II.   95% upper limits on the amplitudes of the neutrino mass at different redshifts reconstructed with a binned parametrization and using different data combinations.

Dataset	CMB	CMB + CMBL	CMB + CMBL + BAO	CMB + CMBL + BAO + SN
$\sum m_\nu(z \leq 0.5)$ (eV)	4.86	3.07	1.73	1.13
$\sum m_\nu(0.5 \leq z \leq 3)$ (eV)	3.19	2.85	0.51	0.42
$\sum m_\nu(3 \leq z \leq 10)$ (eV)	1.64	1.63	0.40	0.37
$\sum m_\nu(10 \leq z \leq 100)$ (eV)	0.47	0.50	0.20	0.19
$\sum m_\nu(100 \leq z \leq 1100)$ (eV)	0.39	0.37	0.33	0.32
$\sum m_\nu(z \geq 1100)$ (eV)	0.44	0.42	0.41	0.40
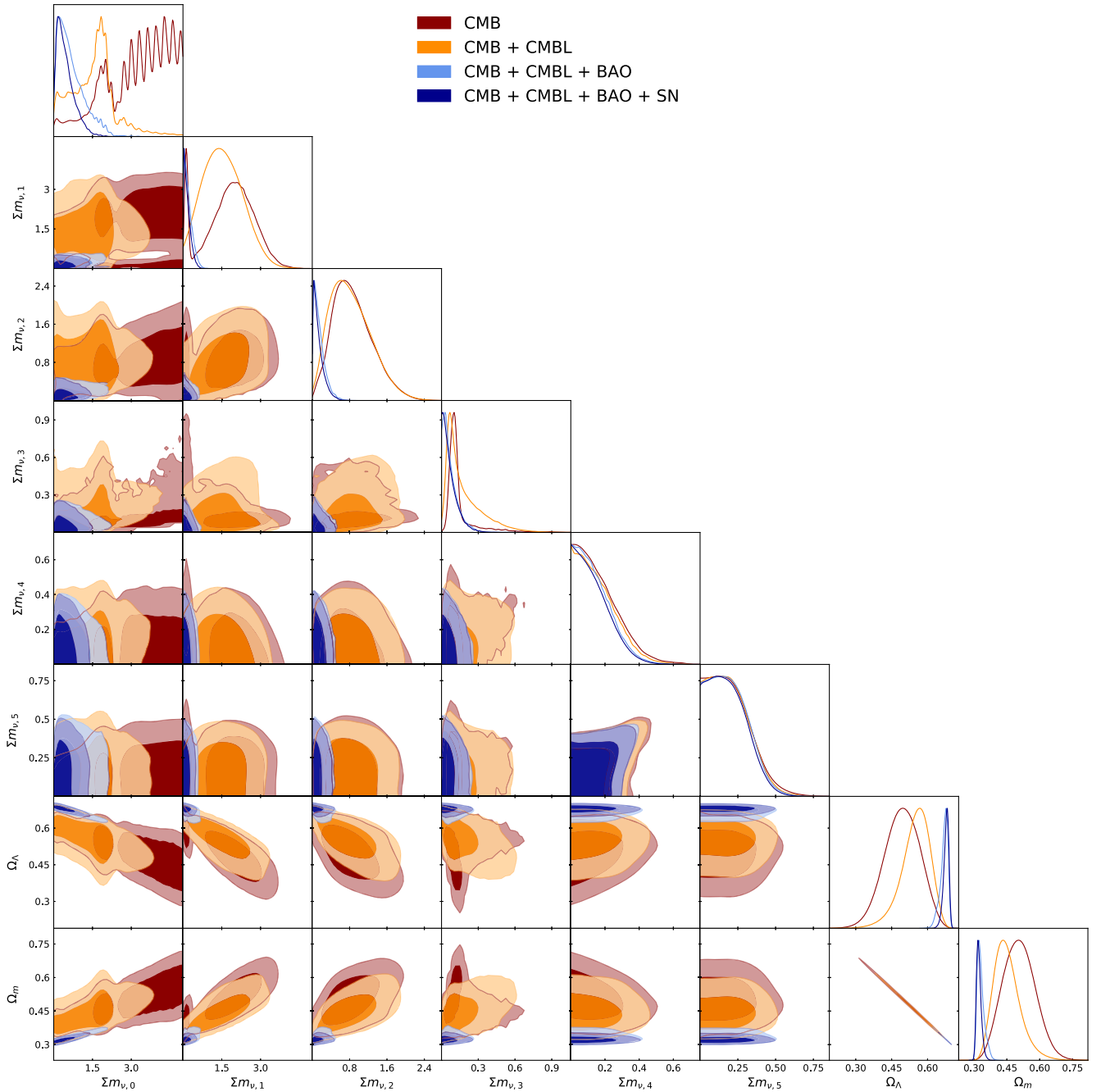
FIG. 2.   2-dimensional contours showing the 68% and 95% CL and 1-dimensional posteriors for the neutrino mass parameters in the individual bins, Ω_Λ and Ω_m. Different colors show different data combinations, as in Fig. 1.

TABLE III. 95% upper limits on the amplitudes of the neutrino mass at different redshifts reconstructed with linear splines and variable knots and using different data combinations.

Dataset	CMB	CMB + CMBL	CMB + CMBL + BAO	CMB + CMBL + BAO + SN
$\sum m_\nu (z=0)$ (eV)	4.75	2.91	1.43	1.46
$\sum m_\nu (z=0.5)$ (eV)	3.50	2.74	2.31	0.76
$\sum m_\nu (z=3)$ (eV)	2.11	1.84	0.18	0.18
$\sum m_\nu (z=10)$ (eV)	1.07	1.11	0.16	0.15
$\sum m_\nu (z=100)$ (eV)	0.69	0.47	0.17	0.18
$\sum m_\nu (z=1100)$ (eV)	0.52	0.50	0.53	0.53

the sum of neutrino masses and the dark energy density might play an important role here.

We note in Fig. 2 that in all cases there is little correlation between the individual neutrino mass amplitudes. We also studied how the inclusion of growth rate measurements obtained with redshift-space distortions (RSD) [128] would affect our results presented here. RSD can be used to probe the growth rate $f(k,z)$ at different scales and redshifts [155]. The scale-dependent feature in this quantity is a source of information for neutrino masses [156–159]. Including the growth rate measurements, we found a decrease of the bound of $\sum m_\nu$ of 38% in the lowest redshift bin and only a marginal improvement in other bins. The exact modeling of RSD is under active development and therefore we present our final results without including RSD.

B. Reconstruction with splines

Next we reconstruct the neutrino mass sum with linear splines and variable knots (see Sec. III). We investigate at which redshift the sensitivity on $\sum m_\nu$ starts to weaken by allowing the knots z_1 and z_2 to vary as well. We show our results for this reconstruction on the right-hand side of Fig. 1. We also present our results in Table III. For the final data combination we find

$$\sum m_\nu (z=0) < 1.46 \text{ eV}$$
$$\sum m_\nu (z=1100) < 0.53 \text{ eV} \quad (95\% \text{ CL}).$$

In general, when comparing the results from the two different reconstruction methods, we note that the constraints for $\sum m_\nu$ at different redshifts are similar. There are small differences, in particular for $\sum m_\nu (z=0)$, because in the binned reconstruction $\sum m_\nu$ is fixed between the bin margins. We also note that, as expected, we obtain smooth curves for the reconstruction with linear splines. This is due to the fact that the positions of the knots z_1 and z_2 are free parameters in the analysis, smoothing the posterior means and credible bands. Compared to the binned reconstruction, we observe that the credible bands of the reconstructed curve via splines with variable knots exhibit more features despite the same number of free parameters.

For constant neutrino masses in time, we would, in principle, expect flat posteriors for the two knots z_1 and z_2, as the position of the knots does not matter when fitting a constant function. However, even in that case, the posterior for z_1 and z_2 can still vary because of possible degeneracies between the neutrino mass sum and other cosmological parameters and because of the different amount of data points at different redshifts, resulting in local changes of the uncertainty of the neutrino mass sum.

In Fig. 3, we see that there is no clear preference for the position of the knots z_1 and z_2. For the position of the first knot (change point) we find $z_1 < 0.89$ (68% CL) for the full data combination. This limit is close to the onset of dark energy domination at $z \sim 0.5$ [160]. The preference for a small value for the position of z_1 is the most pronounced for the final data combination.

The position of the second knot, z_2, is less constrained, but also moves toward lower redshifts when including more data. Whereas the first knot, z_1, mostly is needed to model
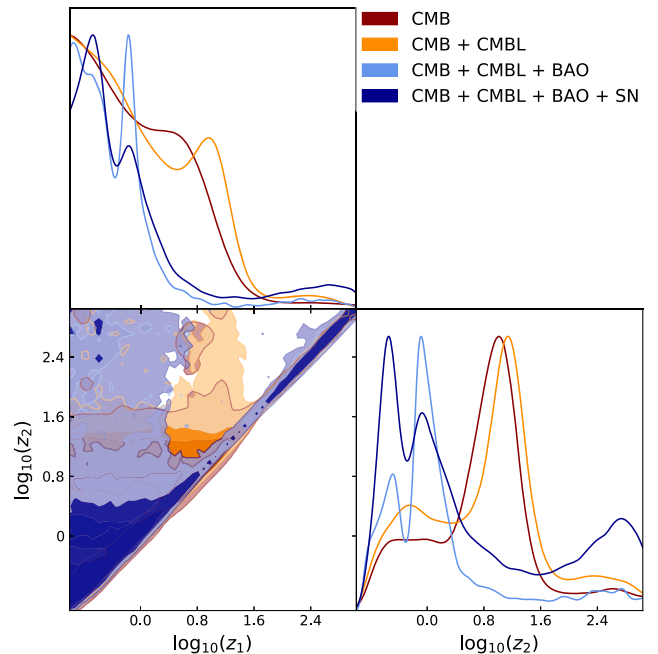

FIG. 3. The results for the change points z_1 and z_2 from the reconstruction with linear splines and variable knots.
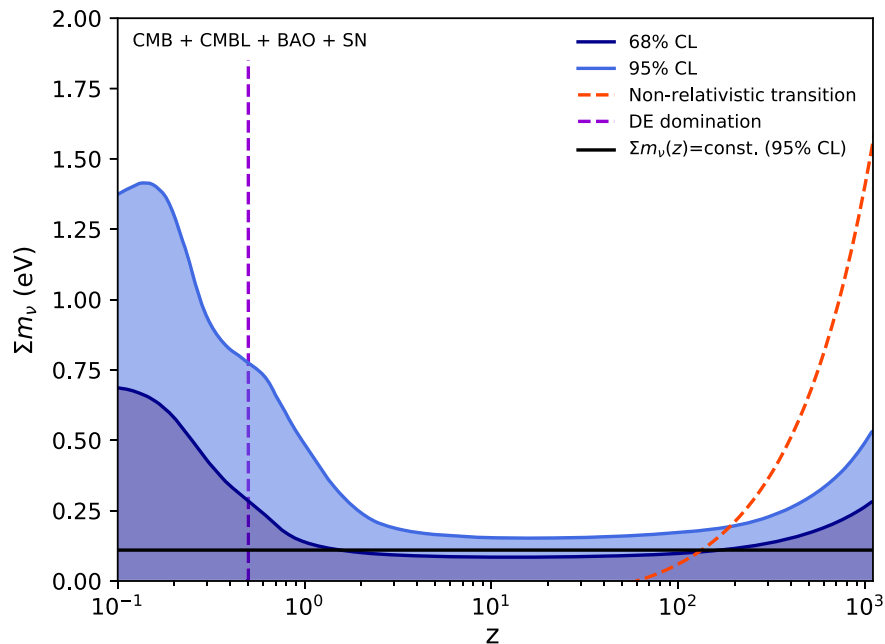
FIG. 4.   Final result: Neutrino mass limits as function of redshift obtained from *Planck* 2018 CMB temperature, polarization, and lensing data, BAO data from BOSS DR12, 6dF, and MGS, eBOSS DR14 quasars, and Lyman-alpha, and SN data from Pantheon 18 (zoom of the lower right-hand panel in Fig. 1). The onset of dark energy domination is denoted with a dashed violet line. The dashed red line shows $\sum m_\nu$ in the case when the neutrino with the largest neutrino mass becomes nonrelativistic at redshift z, assuming a normal neutrino mass hierarchy.

the increase of the uncertainty of $\sum m_\nu(z)$ at low redshifts, the second knot, z_2, determines the width of the regime where the uncertainty of $\sum m_\nu(z)$ is the smallest.

C. Implications for neutrino mass decay models

In this section, we note that our *a priori* model-independent reconstruction can constrain specific models that predict new physics beyond the Standard Model of particle physics. In particular, as discussed in Sec. II B, it has been proposed that neutrinos can decay into dark radiation in the late Universe. To apply our constraints to these models, we need to carefully distinguish two cases. First, in the scenario in which neutrinos decay while they are still relativistic, the anisotropic stress changes before the decay [27]. This makes it hard to directly transfer our bounds to such models, because these models change the neutrino properties both for $z < z_{nr}$ and for $z > z_{nr}$. If instead neutrinos decay after they become nonrelativistic, all cosmological neutrino properties for $z > z_{nr}$ are the same as in the standard case. Thus, any change of neutrino properties for $z < z_{nr}$ due to the decay will not affect the properties for $z > z_{nr}$. In particular, any constraints on cosmological parameters before the decay, such as $\sum m_\nu$ or $\omega_\nu h^2$, will be unaltered in the model compared to the standard ΛCDM model with constant-mass, nondecaying neutrinos. This implies that our constraints for $z > z_{nr}$ can be directly transferred to nonrelativistic neutrino decay models.

Our constraint is shown in our final result plot, Fig. 4, which will be discussed in more detail in the next section. In this plot, the red dashed line is the neutrino mass sum as a function of the redshift z_{nr} at which the largest neutrino mass eigenstate m_{ν_3} becomes nonrelativistic [73],

$$1 + z_{nr} \sim \frac{2m_{\nu_3}}{\text{meV}}, \qquad (3)$$

assuming a normal neutrino mass hierarchy. The smaller neutrino mass eigenstates will become nonrelativistic later and thus can be neglected in this curve. Taking the intersection of the red dashed line and our result curve, we find a limit of

$$\sum m_\nu < 0.21 \text{ eV} \quad (95\% \text{ CL}) \qquad (4)$$

for $z > z_{nr}$. For the nonrelativistic decay scenario, we bound $\sum m_\nu$ with our result for $\sum m_\nu(z = 203)$. Note that $103 < z_{nr} < 203$ are the redshifts at which the individual neutrinos would become nonrelativistic if they had a combined mass of $\sum m_\nu = 0.21$ eV (95% CL) (see Fig. 4).

Using *Planck* 2015 data, it has been previously shown that neutrino decay models can relax the cosmological neutrino mass bound to $\sum m_\nu \lesssim 0.9$ eV for the nonrelativistic decay scenario [23–26]. Note that the cosmological impact of the resulting dark radiation is negligible in these models, as the neutrinos decay during the matter domination era. Compared to the earlier results in [23–26], our

bound in Eq. (4) might be tightened due to two different effects. First, we use more recent CMB data from the latest 2018 *Planck* release [4]. Second, the redshift of the non-relativistic neutrino transition decreases with decreasing neutrino mass, such that the bound gets tighter for later neutrino decays (see Fig. 4). We also note that the neutrino mass bound of $\sum m_\nu \lesssim 0.9$ eV [23–26] relied on simplified assumptions for the equations of motions, as noted in Ref. [27]. This might have an impact on this model-specific mass bound but does not alter our results due to the reasons discussed above.

The limits extracted above do not include all fundamental assumptions of the nonrelativistic decay models, e.g., a decrease in the total neutrino mass. In principle, it is possible that the wider limits that we find at low redshifts could influence the limits at high redshifts. To check the robustness of our estimates, we extended the extraction to include a theoretical prior on the neutrino mass sum with $\sum m_{\nu,z_i} \le \sum m_{\nu,z_j}$ for $z_i \le z_j$. Using this prior, we found an upper limit of $\sum m_\nu < 0.26$ eV (95% CL) for the nonrelativistic decay scenario. This shows that the neutrino mass bound for the decay models is stable with respect to a potential late-time change of the neutrino mass sum.

V. DISCUSSION AND CONCLUSION

In this paper, we reconstructed the cosmological neutrino mass sum as a function of redshift. This reconstruction was model independent, such that no specific mass model or interaction with the dark energy or dark radiation sector was assumed. Our final result is shown in Fig. 4. The figure shows the reconstructed neutrino mass sum for the full data combination of CMB temperature, polarization and lensing, combined with BAO and SN data. We highlight the redshift when dark energy starts to dominate. We also highlight the redshift z_{nr} at which the largest neutrino mass eigenstate becomes nonrelativistic, in order to constrain models [23–26] that predict neutrino decay after this nonrelativistic transition (see Sec. IV and below).

Our result is consistent with neutrino masses that are constant in time, as predicted by the Standard Model of cosmology. We observe a small increase of the bound on $\sum m_\nu$ at high redshifts ($z \gtrsim 500$), as well as a large increase of this bound at low redshifts coinciding with the onset of dark energy domination. The large mass bound at low redshifts could be explained in two different ways.

On the one hand, it could simply arise due to the strong degeneracy between Ω_Λ and $\sum m_\nu$ at low redshifts, which is shown in Fig. 2. We have explicitly tested this scenario by imposing a strong prior on $\Omega_\Lambda = 0.69 \pm 0.01$. In that case, the constraint on $\Sigma m_\nu(z = 0)$ decreased by 42% to $\sum m_\nu(z = 0) = 0.84$ eV, which shows an impact from correlations with dark energy but is still larger than standard neutrino mass bounds. This latter effect might be due to the large number of additional free parameters needed for the reconstruction.

On the other hand, the large mass bound at low redshifts could be explained by new physics. It has been a long-standing puzzle why the energy scales of neutrino masses and dark energy are close ($m_\nu \sim \sqrt[4]{\rho_\Lambda} \sim$ meV) but far away from all other known fundamental energy scales, such as the Higgs or Planck scales. If cosmological data allow for larger neutrino masses in the late Universe, $0 \le z \le 1$ (such as suggested in Refs. [29–36,161]), an intriguing theoretical connection to the dark energy sector could appear [9,28,37–40]. In particular, our results agree with the insights from previous work presented in Ref. [30]. In that study, a specific model was assumed that predicted the late neutrino mass generation in the Universe arising from a supercooled phase transition. We note that our results also show the same trend recently obtained in Ref. [161] by the Dark Energy Survey collaboration, where a higher neutrino mass and a corresponding low Ω_Λ was found.

The analysis presented in this paper could be extended in different ways. On the theory side, it would be interesting to reconstruct $\sum m_\nu(z)$ fully implementing potential interactions with the dark energy or the dark radiation sector (see below). In particular, a coupling between the dark energy and the neutrino sectors would affect the dark energy perturbations, leading to more features in the model and additional ways to decrease the degeneracy between dark energy and massive neutrinos.

Our approach is conservative in the modeling of the neutrino mass but not necessarily in the constraints that we obtain: we choose the simplest parametrization of the mass, without any model-specific assumptions, but the constraints could be weakened or strengthened when model-specific physics is introduced. For example, the neutrino mass bounds could become much weaker for modified gravity models [10–12] or when introducing a nontrivial coupling between the neutrino and dark energy sectors, for example in the model considered in Ref. [30]. On the other hand, the bounds are expected to become stronger in neutrino decay models when taking into account neutrino perturbations [23–26]. Such features could be captured by a more general reconstruction of the neutrino mass including nontrivial couplings to different sectors.

On the methodology side, one could model the number of knots or bins with a hyperparameter [138] in order to allow the data to decide on the number of knots. To speed up computations, this can be fitted with empirical Bayes, where the hyperparameters are chosen as the maximizers of the marginalized likelihood [58,162]. The exact number of knots or bins can impact the results by under- or overfitting the reconstructed function.

On the data side, it would be interesting to reconstruct $\sum m_\nu$ including more large scale structure data, in particular galaxy clustering, cosmic shear, and cross-correlations of either the ℓISW effect and galaxy clustering or of CMB lensing and tracers of the large scale

structure. These additional measurements of the suppression of the matter power spectrum would also be an additional way to break the degeneracy with dark energy (see, e.g., [43,83,114,163–170]). To fully exploit these data will however require careful modeling of the nonlinear scales (see, e.g., [171–180]), and of potential systematics, such as the scale-dependent galaxy bias in the presence of massive neutrinos [149,181–184].

Finally, we comment on the implications of our results for particle physics models and experiments. In particular, our study strengthens the previously reported cosmological mass bound $\sum m_\nu < 0.9$ eV (95% CL) of nonrelativistic neutrino mass decay scenarios [23–26] to $\sum m_\nu < 0.21$ eV (95% CL). We note that the constraints are still weaker than for constant neutrino masses in time, because decay scenarios are insensitive to late-time cosmological data from BAO and SN. However, our study pushes the neutrino mass bounds of such models below the sensitivity of the KATRIN experiment. This implies that a neutrino mass discovery at KATRIN would hint toward other models, such as models predicting post-recombination neutrino mass generation and subsequent relic neutrino annihilation, such as proposed in Ref. [9]. The cosmological disappearance of the neutrino mass parameter might also be explained in the context of modified gravity [10–12], but this degeneracy between massive neutrino and modify gravity effects will be broken by future surveys, such as Euclid [12].

[1] P. A. Zyla *et al.* (Particle Data Group), Review of particle physics, Prog. Theor. Exp. Phys. **2020** (2020).

[2] M. Aker *et al.*, First direct neutrino-mass measurement with sub-eV sensitivity, arXiv:2105.08533.

[3] M. Aker *et al.*, Analysis methods for the first KATRIN neutrino-mass measurement, Phys. Rev. D **104**, 012005 (2021).

[4] N. Aghanim *et al.* (Planck Collaboration), Planck 2018 results. VI. Cosmological parameters, Astron. Astrophys. **641**, A6 (2020).

[5] J. F. Beacom, N. F. Bell, and S. Dodelson, Neutrinoless Universe, Phys. Rev. Lett. **93**, 121302 (2004).

[6] S. Hannestad, Structure formation with strongly interacting neutrinos—Implications for the cosmological neutrino mass bound, J. Cosmol. Astropart. Phys. 02 (2005) 011.

[7] L. Lancaster, F.-Y. Cyr-Racine, L. Knox, and Z. Pan, A tale of two modes: Neutrino free-streaming in the early universe, J. Cosmol. Astropart. Phys. 07 (2017) 033.

[8] B. Follin, L. Knox, M. Millea, and Z. Pan, First Detection of the Acoustic Oscillation Phase Shift Expected from the Cosmic Neutrino Background, Phys. Rev. Lett. **115**, 091301 (2015).

[9] G. Dvali and L. Funcke, Small neutrino masses from gravitational θ-term, Phys. Rev. D **93**, 113002 (2016).

[10] N. Bellomo, E. Bellini, B. Hu, R. Jimenez, C. Pena-Garay, and L. Verde, Hiding neutrino mass in modified gravity cosmologies, J. Cosmol. Astropart. Phys. 02 (2017) 043.

[11] S. Hagstotz, M. Gronke, D. Mota, and M. Baldi, Breaking cosmic degeneracies: Disentangling neutrinos and modified gravity with kinematic information, Astron. Astrophys. **629**, A46 (2019).

[12] S. Hagstotz, M. Costanzi, M. Baldi, and J. Weller, Joint halo-mass function for modified gravity and massive neutrinos I. Simulations and cosmological forecasts, Mon. Not. R. Astron. Soc. **486**, 3927 (2019).

[13] I. Esteban and J. Salvado, Long range interactions in cosmology: Implications for neutrinos, J. Cosmol. Astropart. Phys. 05 (2021) 036.

[14] S. Joudaki and M. Kaplinghat, Dark energy and neutrino masses from future measurements of the expansion history and growth of structure, Phys. Rev. D **86**, 023526 (2012).

[15] S. Joudaki, Constraints on neutrino mass and light degrees of freedom in extended cosmological parameter spaces, Phys. Rev. D **87**, 083523 (2013).

[16] R. Allison, P. Caucal, E. Calabrese, J. Dunkley, and T. Louis, Towards a cosmological neutrino mass detection, Phys. Rev. D **92**, 123535 (2015).

[17] C. S. Lorenz, E. Calabrese, and D. Alonso, Distinguishing between neutrinos and time-varying dark energy through cosmic time, Phys. Rev. D **96,** 043510 (2017).

[18] W. Yang, R. C. Nunes, S. Pan, and D. F. Mota, Effects of neutrino mass hierarchies on dynamical dark energy models, Phys. Rev. D **95,** 103522 (2017).

[19] S. Vagnozzi, S. Dhawan, M. Gerbino, K. Freese, A. Goobar, and O. Mena, Constraints on the sum of the neutrino masses in dynamical dark energy models with $w(z) \geq -1$ are tighter than those obtained in ΛCDM, Phys. Rev. D **98,** 083501 (2018).

[20] S. Roy Choudhury and S. Choubey, Updated bounds on sum of neutrino masses in various cosmological scenarios, J. Cosmol. Astropart. Phys. 09 (2018) 017.

[21] S. Roy Choudhury and S. Hannestad, Updated results on neutrino mass and mass hierarchy from cosmology with Planck 2018 likelihoods, J. Cosmol. Astropart. Phys. 07 (2020) 037.

[22] I. M. Oldengott, G. Barenboim, S. Kahlen, J. Salvado, and D. J. Schwarz, How to relax the cosmological neutrino mass bound, J. Cosmol. Astropart. Phys. 04 (2019) 049.

[23] M. Escudero and M. Fairbairn, Cosmological constraints on invisible neutrino decays revisited, Phys. Rev. D **100,** 103531 (2019).

[24] Z. Chacko, A. Dev, P. Du, V. Poulin, and Y. Tsai, Cosmological limits on the neutrino mass and lifetime, J. High Energy Phys. 04 (2020) 020.

[25] Z. Chacko, A. Dev, P. Du, V. Poulin, and Y. Tsai, Determining the neutrino lifetime from cosmology, Phys. Rev. D **103,** 043519 (2021).

[26] M. Escudero, J. Lopez-Pavon, N. Rius, and S. Sandner, Relaxing cosmological neutrino mass bounds with unstable neutrinos, J. High Energy Phys. 12 (2020) 119.

[27] Ga. Barenboim, J. Z. Chen, S. Hannestad, I. M. Oldengott, T. Tram, and Y. Y. Y. Wong, Invisible neutrino decay in precision cosmology, J. Cosmol. Astropart. Phys. 03 (2021) 087.

[28] R. Fardon, A. E. Nelson, and N. Weiner, Dark energy from mass varying neutrinos, J. Cosmol. Astropart. Phys. 10 (2004) 005.

[29] S. M. Koksbang and S. Hannestad, Constraining dynamical neutrino mass generation with cosmological data, J. Cosmol. Astropart. Phys. 09 (2017) 014.

[30] C. S. Lorenz, L. Funcke, E. Calabrese, and S. Hannestad, Time-varying neutrino mass from a supercooled phase transition: Current cosmological constraints and impact on the $\Omega_m - \sigma_8$ plane, Phys. Rev. D **99,** 023501 (2019).

[31] A. W. Brookfield, C. van de Bruck, D. F. Mota, and D. Tocchini-Valentini, Cosmology with Massive Neutrinos Coupled to Dark Energy, Phys. Rev. Lett. **96,** 061301 (2006).

[32] A. W. Brookfield, C. van de Bruck, D. F. Mota, and D. Tocchini-Valentini, Cosmology of mass-varying neutrinos driven by quintessence: Theory and observations, Phys. Rev. D **73,** 083515 (2006).

[33] R. A. Battye and A. Moss, Evidence for Massive Neutrinos from Cosmic Microwave Background and Lensing Observations, Phys. Rev. Lett. **112,** 051303 (2014).

[34] M. Wyman, D. H. Rudd, R. A. Vanderveld, and W. Hu, Neutrinos Help Reconcile Planck Measurements with the Local Universe, Phys. Rev. Lett. **112,** 051302 (2014).

[35] F. Beutler *et al.* (BOSS Collaboration), The clustering of galaxies in the SDSS-III baryon oscillation spectroscopic survey: Signs of neutrino mass in current cosmological data sets, Mon. Not. R. Astron. Soc. **444,** 3501 (2014).

[36] V. Poulin, K. K. Boddy, S. Bird, and M. Kamionkowski, Implications of an extended dark energy cosmology with massive neutrinos for cosmological tensions, Phys. Rev. D **97,** 123504 (2018).

[37] O. E. Bjaelde, A. W. Brookfield, C. van de Bruck, S. Hannestad, D. F. Mota, L. Schrempp, and D. Tocchini-Valentini, Neutrino dark energy—revisiting the stability issue, J. Cosmol. Astropart. Phys. 01 (2008) 026.

[38] Y. Ayaita, M. Baldi, F. Fhrer, E. Puchwein, and C. Wetterich, Nonlinear growing neutrino cosmology, Phys. Rev. D **93,** 063511 (2016).

[39] S. Mandal, G. Y. Chitov, O. Avsajanishvili, B. Singha, and T. Kahniashvili, Mass varying neutrinos with different quintessence potentials, J. Cosmol. Astropart. Phys. 05 (2021) 018.

[40] G. D'Amico, T. Hamill, and N. Kaloper, Neutrino masses from outer space, Phys. Lett. B **797,** 134846 (2019).

[41] G. Drexlin, V. Hannen, S. Mertens, and C. Weinheimer, Current direct neutrino mass experiments, Adv. High Energy Phys. **2013,** 293986 (2013).

[42] K. N. Abazajian *et al.*, Neutrino physics from the cosmic microwave background and large scale structure, Astropart. Phys. **63,** 66 (2015).

[43] S. Mishra-Sharma, D. Alonso, and J. Dunkley, Neutrino masses and beyond- ΛCDM cosmology with LSST and future CMB experiments, Phys. Rev. D **97,** 123544 (2018).

[44] T. Holsclaw, U. Alam, B. Sansó, H. Lee, K. Heitmann, S. Habib, and D. Higdon, Nonparametric Dark Energy Reconstruction from Supernova Data, Phys. Rev. Lett. **105,** 241302 (2010).

[45] T. Holsclaw, U. Alam, B. Sansó, H. Lee, K. Heitmann, S. Habib, and D. Higdon, Nonparametric reconstruction of the dark energy equation of state from diverse data sets, Phys. Rev. D **84,** 083501 (2011).

[46] M. Seikel, C. Clarkson, and M. Smith, Reconstruction of dark energy and expansion dynamics using Gaussian processes, J. Cosmol. Astropart. Phys. 06 (2012) 036.

[47] M. Seikel and C. Clarkson, Optimising Gaussian processes for reconstructing dark energy dynamics from supernovae, arXiv:1311.6678.

[48] J. Alberto Vazquez, M. Bridges, M. P. Hobson, and A. N. Lasenby, Reconstruction of the dark energy equation of state, J. Cosmol. Astropart. Phys. 09 (2012) 020.

[49] A. Montiel, R. Lazkoz, I. Sendra, C. Escamilla-Rivera, and V. Salzano, Nonparametric reconstruction of the cosmic expansion with local regression smoothing and simulation extrapolation, Phys. Rev. D **89,** 043007 (2014).

[50] S. Hee, W. Handley, M. P. Hobson, and A. N. Lasenby, Bayesian model selection without evidences: Application to the dark energy equation-of-state, Mon. Not. R. Astron. Soc. **455,** 2461 (2016).

[51] S. Hee, J. A. Vzquez, W. J. Handley, M. P. Hobson, and A. N. Lasenby, Constraining the dark energy equation

of state using Bayes theorem and the KullbackLeibler divergence, Mon. Not. R. Astron. Soc. **466,** 369 (2017).

[52] F. Gerardi, M. Martinelli, and A. Silvestri, Reconstruction of the dark energy equation of state from latest data: The impact of theoretical priors, J. Cosmol. Astropart. Phys. 07 (2019) 042.

[53] S. Joudaki, M. Kaplinghat, R. Keeley, and D. Kirkby, Model independent inference of the expansion history and implications for the growth of structure, Phys. Rev. D **97,** 123501 (2018).

[54] R. E. Keeley, S. Joudaki, M. Kaplinghat, and D. Kirkby, Implications of a transition in the dark energy equation of state for the H_0 and σ_8 tensions, J. Cosmol. Astropart. Phys. 12 (2019) 035.

[55] M. Park, M. Raveri, and B. Jain, Reconstructing quintessence, Phys. Rev. D **103,** 103530 (2021).

[56] A. Bonilla, S. Kumar, R. C. Nunes, and S. Pan, Reconstruction of the dark sectors' interaction: A model-independent inference and forecast from GW standard sirens, arXiv:2102.06149.

[57] A. Shafieloo, A. G. Kim, and E. V. Linder, Gaussian process cosmography, Phys. Rev. D **85,** 123530 (2012).

[58] M. Seikel, S. Yahya, R. Maartens, and C. Clarkson, Using H(z) data as a probe of the concordance model, Phys. Rev. D **86,** 083001 (2012).

[59] J. L. Bernal, L. Verde, and A. G. Riess, The trouble with H_0, J. Cosmol. Astropart. Phys. 10 (2016) 019.

[60] A. Gómez-Valent and L. Amendola, H_0 from cosmic chronometers and type Ia supernovae, with Gaussian processes and the novel weighted polynomial regression method, J. Cosmol. Astropart. Phys. 04 (2018) 051.

[61] F. Renzi and A. Silvestri, A Look at the Hubble Speed from First Principles, arXiv:2011.10559 [Phys. Rev. Lett. (to be published)].

[62] José Luis Bernal, Licia Verde, Raul Jimenez, Marc Kamionkowski, David Valcin, and Benjamin D. Wandelt, The trouble beyond H_0 and the new cosmic triangles, Phys. Rev. D **103,** 103533 (2021).

[63] S. L. Bridle, A. M. Lewis, J. Weller, and G. Efstathiou, Reconstructing the primordial power spectrum, Mon. Not. R. Astron. Soc. **342,** L72 (2003).

[64] Zong-Kuan Guo, Dominik J. Schwarz, and Yuan-Zhong Zhang, Reconstruction of the primordial power spectrum from CMB data, J. Cosmol. Astropart. Phys. 08 (2011) 031.

[65] D. K. Hazra, A. Shafieloo, and T. Souradeep, Primordial power spectrum from Planck, J. Cosmol. Astropart. Phys. 11 (2014) 011.

[66] P. Hunt and S. Sarkar, Reconstruction of the primordial power spectrum of curvature perturbations using multiple data sets, J. Cosmol. Astropart. Phys. 01 (2014) 025.

[67] B. Lévy, R. Mohayaee, and S. von Hausegger, A fast semi-discrete optimal transport algorithm for a unique reconstruction of the early Universe, Mon. Not. R. Astron. Soc. **506,** 1165 (2021).

[68] C. Garcia-Quintero, M. Ishak, and O. Ning, Current constraints on deviations from general relativity using binning in redshift and scale, J. Cosmol. Astropart. Phys. 12 (2020) 018.

[69] L. Verde, T. Treu, and A. G. Riess, Tensions between the early and the late Universe, Nat. Astron. **3,** 891 (2019).

[70] M. Kunz, The dark degeneracy: On the number and nature of dark components, Phys. Rev. D **80,** 123001 (2009).

[71] L. Amendola, M. Kunz, M. Motta, I. D. Saltas, and I. Sawicki, Observables and unobservables in dark energy cosmologies, Phys. Rev. D **87,** 023501 (2013).

[72] V. C. Busti and C. Clarkson, Dodging the dark matter degeneracy while determining the dynamics of dark energy, J. Cosmol. Astropart. Phys. 05 (2016) 008.

[73] K. Ichikawa, M. Fukugita, and M. Kawasaki, Constraining neutrino masses by CMB experiments alone, Phys. Rev. D **71,** 043001 (2005).

[74] M. Archidiacono, T. Brinckmann, J. Lesgourgues, and V. Poulin, Physical effects involved in the measurements of neutrino masses with future cosmological data, J. Cosmol. Astropart. Phys. 02 (2017) 052.

[75] J. Lesgourgues, G. Mangano, G. Miele, and S. Pastor, *Neutrino Cosmology* (Cambridge University Press, Cambridge, England, 2013).

[76] S. Vagnozzi, E. Giusarma, O. Mena, K. Freese, M. Gerbino, S. Ho, and M. Lattanzi, Unveiling ν secrets with cosmological data: Neutrino masses and mass hierarchy, Phys. Rev. D **96,** 123503 (2017).

[77] C. Howlett, A. Lewis, A. Hall, and A. Challinor, CMB power spectrum parameter degeneracies in the era of precision cosmology, J. Cosmol. Astropart. Phys. 04 (2012) 027.

[78] W. Sutherland, The CMB neutrino mass/vacuum energy degeneracy: A simple derivation of the degeneracy slopes, Mon. Not. R. Astron. Soc. **477,** 1913 (2018).

[79] M. Moresco, L. Verde, L. Pozzetti, R. Jimenez, and A. Cimatti, New constraints on cosmological parameters and neutrino properties using the expansion rate of the Universe to $z \sim 1.75$, J. Cosmol. Astropart. Phys. 07 (2012) 053.

[80] A. C. Hall and A. Challinor, Probing the neutrino mass hierarchy with cosmic microwave background weak lensing, Mon. Not. R. Astron. Soc. **425,** 1170 (2012).

[81] G. Cabass, M. Gerbino, E. Giusarma, A. Melchiorri, L. Pagano, and L. Salvati, Constraints on the early and late integrated Sachs-Wolfe effects from the Planck 2015 cosmic microwave background anisotropies in the angular power spectra, Phys. Rev. D **92,** 063534 (2015).

[82] Z. Hou, C. L. Reichardt, K. T. Story, B. Follin, Keisler *et al.*, Constraints on cosmology from the cosmic microwave background power spectrum of the 2500 deg^2 SPT-SZ survey, Astrophys. J. **782,** 74 (2014).

[83] J. Lesgourgues, W. Valkenburg, and E. Gaztanaga, Constraining neutrino masses with the ISW-galaxy correlation function, Phys. Rev. D **77,** 063505 (2008).

[84] A. Lewis and A. Challinor, Weak gravitational lensing of the CMB, Phys. Rep. **429,** 1 (2006).

[85] J. Lesgourgues and S. Pastor, Massive neutrinos and cosmology, Phys. Rep. **429,** 307 (2006).

[86] W. Hu, D. J. Eisenstein, and M. Tegmark, Weighing Neutrinos with Galaxy Surveys, Phys. Rev. Lett. **80,** 5255 (1998).

[87] J. W. Henning *et al.* (SPT Collaboration), Measurements of the temperature and E-mode polarization of the CMB from 500 square degrees of SPTpol data, Astrophys. J. **852,** 97 (2018).

[88] N. Aghanim *et al.* (Planck Collaboration), Planck 2018 results. V. CMB power spectra and likelihoods, Astron. Astrophys. **641,** A5 (2020).

[89] S. K. Choi *et al.* (ACT Collaboration), The atacama cosmology telescope: A measurement of the cosmic microwave background power spectra at 98 and 150 GHz, J. Cosmol. Astropart. Phys. 12 (2020) 045.

[90] F. Bianchini *et al.* (SPT Collaboration), Constraints on cosmological parameters from the 500 deg^2 SPTpol lensing power spectrum, Astrophys. J. **888,** 119 (2020).

[91] O. Darwish *et al.*, The atacama cosmology telescope: A CMB lensing mass map over 2100 square degrees of sky and its cross-correlation with BOSS-CMASS galaxies, Mon. Not. R. Astron. Soc. **500,** 2250 (2020).

[92] E. Calabrese, D. Alonso, and J. Dunkley, Complementing the ground-based CMB-S4 experiment on large scales with the PIXIE satellite, Phys. Rev. D **95,** 063504 (2017).

[93] D. J. Eisenstein *et al.* (SDSS Collaboration), Detection of the baryon acoustic peak in the large-scale correlation function of SDSS luminous red galaxies, Astrophys. J. **633,** 560 (2005).

[94] S. Cole *et al.* (2dFGRS Collaboration), The 2dF galaxy redshift survey: Power-spectrum analysis of the final dataset and cosmological implications, Mon. Not. R. Astron. Soc. **362,** 505 (2005).

[95] D. H. Weinberg, M. J. Mortonson, D. J. Eisenstein, C. Hirata, A. G. Riess, and E. Rozo, Observational probes of cosmic acceleration, Phys. Rep. **530,** 87 (2013).

[96] B. A. Bassett and R. Hlozek, Baryon acoustic oscillations, arXiv:0910.5224.

[97] S. Alam *et al.* (eBOSS Collaboration), The completed SDSS-IV extended baryon oscillation spectroscopic survey: Cosmological implications from two decades of spectroscopic surveys at the apache point observatory, Phys. Rev. D **103,** 083533 (2021).

[98] E. de Carvalho, A. Bernui, G. C. Carvalho, C. P. Novaes, and H. S. Xavier, Angular baryon acoustic oscillation measure at $z = 2.225$ from the SDSS quasar survey, J. Cosmol. Astropart. Phys. 04 (2018) 064.

[99] M. Ata *et al.*, The clustering of the SDSS-IV extended baryon oscillation spectroscopic survey DR14 quasar sample: First measurement of baryon acoustic oscillations between redshift 0.8 and 2.2, Mon. Not. R. Astron. Soc. **473,** 4773 (2018).

[100] J. Hou, A. G. Sánchez, A. J. Ross, A. Smith, R. Neveux *et al.*, The completed SDSS-IV extended baryon oscillation spectroscopic survey: BAO and RSD measurements from anisotropic clustering analysis of the quasar sample in configuration space between redshift 0.8 and 2.2, Mon. Not. R. Astron. Soc. **500,** 1201 (2020).

[101] P. McDonald and D. Eisenstein, Dark energy and curvature from a future baryonic acoustic oscillation survey using the Lyman-alpha forest, Phys. Rev. D **76,** 063009 (2007).

[102] J. E. Bautista *et al.*, Measurement of baryon acoustic oscillation correlations at $z = 2.3$ with SDSS DR12 Lyα-forests, Astron. Astrophys. **603,** A12 (2017).

[103] U. Seljak *et al.* (SDSS Collaboration), Cosmological parameter analysis including SDSS Ly-alpha forest and galaxy bias: Constraints on the primordial spectrum of fluctuations, neutrino mass, and dark energy, Phys. Rev. D **71,** 103515 (2005).

[104] U. Seljak, A. Slosar, and P. McDonald, Cosmological parameters from combining the Lyman-alpha forest with CMB, galaxy clustering and SN constraints, J. Cosmol. Astropart. Phys. 10 (2006) 014.

[105] N. Palanque-Delabrouille *et al.*, Constraint on neutrino masses from SDSS-III/BOSS Lyα forest and other cosmological probes, J. Cosmol. Astropart. Phys. 02 (2015) 045.

[106] N. Palanque-Delabrouille *et al.*, Neutrino masses and cosmology with Lyman-alpha forest power spectrum, J. Cosmol. Astropart. Phys. 11 (2015) 011.

[107] N. Palanque-Delabrouille, C. Yèche, N. Schöneberg, J. Lesgourgues, M. Walther, S. Chabanier, and E. Armengaud, Hints, neutrino bounds and WDM constraints from SDSS DR14 Lyman-α and Planck full-survey data, J. Cosmol. Astropart. Phys. 04 (2020) 038.

[108] R. A. C. Croft, D. H. Weinberg, N. Katz, and L. Hernquist, Recovery of the power spectrum of mass fluctuations from observations of the lyα forest, Astrophys. J. **495,** 44 (1998).

[109] H. Zhan, R. Dave, D. Eisenstein, and N. Katz, Ly-alpha flux power spectrum and its covariance, Mon. Not. R. Astron. Soc. **363,** 1145 (2005).

[110] C. Pedersen, A. Font-Ribera, T. D. Kitching, P. McDonald, S. Bird, A. Slosar, K. K. Rogers, and A. Pontzen, Massive neutrinos and degeneracies in Lyman-alpha forest simulations, J. Cosmol. Astropart. Phys. 04 (2020) 025.

[111] L. Hui and N. Y. Gnedin, Equation of state of the photo-ionized intergalactic medium, Mon. Not. R. Astron. Soc. **292,** 27 (1997).

[112] M. Walther, E. Armengaud, C. Ravoux, N. Palanque-Delabrouille, C. Yèche, and Z. Lukić, Simulating intergalactic gas for DESI-like small scale Lymanα forest observations, J. Cosmol. Astropart. Phys. 04 (2021) 059.

[113] A. Goobar and B. Leibundgut, Supernova cosmology: Legacy and future, Annu. Rev. Nucl. Part. Sci. **61,** 251 (2011).

[114] A. Boyle, Understanding the neutrino mass constraints achievable by combining CMB lensing and spectroscopic galaxy surveys, J. Cosmol. Astropart. Phys. 04 (2019) 038; Erratum, 10 (2019) 01.

[115] P. Minkowski, e at a rate of one out of 109 muon decays?, Phys. Lett. **67B,** 421 (1977).

[116] M. Gell-Mann, P. Ramond, and R. Slansky, in *Proceedings of the Supergravity Stony Brook Workshop*, edited by P. Van Nieuwenhuizen and D. Freedman (Elsevier, Amsterdam, 1979).

[117] T. Yanagida, Horizontal symmetry and masses of neutrinos, Prog. Theor. Phys. **64,** 1103 (1980).

[118] R. N. Mohapatra and G. Senjanović, Neutrino Mass and Spontaneous Parity Nonconservation, Phys. Rev. Lett. **44,** 912 (1980).

[119] J. Schechter and J. W. F. Valle, Neutrino masses in su(2) ⊗ u(1) theories, Phys. Rev. D **22,** 2227 (1980).

[120] J. Schechter and J. W. F. Valle, Neutrino decay and spontaneous violation of lepton number, Phys. Rev. D **25**, 774 (1982).

[121] N. Afshordi, M. Zaldarriaga, and K. Kohri, On the stability of dark energy with mass-varying neutrinos, Phys. Rev. D **72**, 065024 (2005).

[122] G. Dvali and L. Funcke, Domestic axion, arXiv:1608.08969.

[123] L. Funcke, G. Raffelt, and E. Vitagliano, Distinguishing dirac and Majorana neutrinos by their decays via Nambu-Goldstone bosons in the gravitational-anomaly model of neutrino masses, Phys. Rev. D **101**, 015025 (2020).

[124] M. G. Betti, M. Biasotti, A. Bosc, F. Calle, N. Canci, G. Cavoto, C. Chang, A. G. Cocco, A. P. Colijn, J. Conrad *et al.*, Neutrino physics with the ptolemy project: Active neutrino properties and the light sterile case, J. Cosmol. Astropart. Phys. 07 (2019) 047.

[125] P. A. R. Ade *et al.* (Planck Collaboration), Planck 2015 results. XIII. Cosmological parameters, Astron. Astrophys. **594**, A13 (2016).

[126] F. Beutler, C. Blake, M. Colless, D. H. Jones, L. Staveley-Smith, L. Campbell, Q. Parker, W. Saunders, and F. Watson, The 6dF galaxy survey: Baryon acoustic oscillations and the local Hubble constant, Mon. Not. R. Astron. Soc. **416**, 3017 (2011).

[127] A. J. Ross, L. Samushia, C. Howlett, W. J. Percival, A. Burden, and M. Manera, The clustering of the SDSS DR7 main Galaxy sample—I. A 4 per cent distance measure at $z = 0.15$, Mon. Not. R. Astron. Soc. **449**, 835 (2015).

[128] S. Alam *et al.* (BOSS Collaboration), The clustering of galaxies in the completed SDSS-III baryon oscillation spectroscopic survey: Cosmological analysis of the DR12 galaxy sample, Mon. Not. R. Astron. Soc. **470**, 2617 (2017).

[129] M. Blomqvist *et al.*, Baryon acoustic oscillations from the cross-correlation of Lyα absorption and quasars in eBOSS DR14, Astron. Astrophys. **629**, A86 (2019).

[130] N. Schneberg, J. Lesgourgues, and D. C. Hooper, The BAO + BBN take on the Hubble tension, J. Cosmol. Astropart. Phys. 10 (2019) 029.

[131] D. M. Scolnic, D. O. Jones, A. Rest, Y. C. Pan, R. Chornock, R. J. Foley, M. E. Huber, R. Kessler, G. Narayan, A. G. Riess *et al.*, The complete light-curve sample of spectroscopically confirmed sne ia from pan-starrs1 and cosmological constraints from the combined pantheon sample, Astrophys. J. **859**, 101 (2018).

[132] N. Aghanim *et al.* (Planck Collaboration), Planck 2018 results. VIII. Gravitational lensing, Astron. Astrophys. **641**, A8 (2020).

[133] A. Lewis, A. Challinor, and A. Lasenby, Efficient computation of CMB anisotropies in closed FRW models, Astrophys. J. **538**, 473 (2000).

[134] A. Lewis and S. Bridle, Cosmological parameters from CMB and other data: A Monte Carlo approach, Phys. Rev. D **66**, 103511 (2002).

[135] L. Wasserman, *All of Nonparametric Statistics* (Springer-Verlag, New York, 2006).

[136] C. Carbone, V. Springel, C. Baccigalupi, M. Bartelmann, and S. Matarrese, Full-sky maps for gravitational lensing of the CMB, Mon. Not. R. Astron. Soc. **388**, 1618 (2008).

[137] M. Muccino, L. Izzo, O. Luongo, K. Boshkayev, L. Amati, M. Della Valle, G. B. Pisani, and E. Zaninoni, Tracing dark energy history with gamma ray bursts, Astrophys. J. **908**, 181 (2021).

[138] C. R. Genovese, I. Dimatteo, and R. E. Kass, Bayesian curvefitting with freeknot splines, Biometrika **88**, 1055 (2001).

[139] J. Alberto Vázquez, M. Bridges, M. P. Hobson, and A. N. Lasenby, Model selection applied to reconstruction of the primordial power spectrum, J. Cosmol. Astropart. Phys. 06 (2012) 006.

[140] M. Millea and F. Bouchet, Cosmic microwave background constraints in light of priors over reionization histories, Astron. Astrophys. **617**, A96 (2018).

[141] A. Lewis, GetDist: A Python package for analysing Monte Carlo samples, arXiv:1910.13970.

[142] S. Gariazzo, M. Archidiacono, P. F. de Salas, O. Mena, C. A. Ternes, and M. Tórtola, Neutrino masses and their ordering: Global data, priors and models, J. Cosmol. Astropart. Phys. 03 (2018) 011.

[143] C. Pena-Garay and L. Verde, Can we measure the neutrino mass hierarchy in the sky?, J. Cosmol. Astropart. Phys. 05 (2010) 035.

[144] M. Gerbino, M. Lattanzi, O. Mena, and K. Freese, A novel approach to quantifying the sensitivity of current and future cosmological datasets to the neutrino mass ordering through Bayesian hierarchical modeling, Phys. Lett. B **775**, 239 (2017).

[145] M. Lattanzi and M. Gerbino, Status of neutrino properties and future prospects—Cosmological and astrophysical constraints, Front. Phys. **5**, 70 (2018).

[146] P. F. De Salas, S. Gariazzo, O. Mena, C. A. Ternes, and M. Tórtola, Neutrino mass ordering from oscillations and beyond: 2018 Status and future prospects, Front. Astron. Space Sci. **5**, 36 (2018).

[147] C. Mahony, B. Leistedt, H. V. Peiris, J. Braden, B. Joachimi, A. Korn, L. Cremonesi, and R. Nichol, Target neutrino mass precision for determining the neutrino hierarchy, Phys. Rev. D **101**, 083513 (2020).

[148] M. Archidiacono, S. Hannestad, and J. Lesgourgues, What will it take to measure individual neutrino mass states using cosmology?, J. Cosmol. Astropart. Phys. 09 (2020) 021.

[149] W. L. Xu, N. DePorzio, J. B. Muñoz, and C. Dvorkin, Accurately weighing neutrinos with cosmological surveys, Phys. Rev. D **103**, 023503 (2021).

[150] P. Stöcker *et al.* (GAMBIT Cosmology Workgroup Collaboration), Strengthening the bound on the mass of the lightest neutrino with terrestrial and cosmological experiments, Phys. Rev. D **103**, 123508 (2021).

[151] L. T. Hergt, W. J. Handley, M. P. Hobson, and A. N. Lasenby, Bayesian evidence for the tensor-to-scalar ratio r and neutrino masses m_ν: Effects of uniform vs logarithmic priors, Phys. Rev. D **103**, 123511 (2021).

[152] F. Hassani, S. Baghram, and H. Firouzjahi, Lensing as a probe of early Universe: From CMB to galaxies, J. Cosmol. Astropart. Phys. 05 (2016) 044.

[153] A. Manzotti, Future cosmic microwave background delensing with galaxy surveys, Phys. Rev. D **97**, 043527 (2018).

[154] B. D. Sherwin, J. Dunkley, S. Das *et al.*, Evidence for Dark Energy from the Cosmic Microwave Background Alone Using the Atacama Cosmology Telescope Lensing Measurements, Phys. Rev. Lett. **107,** 021302 (2011).

[155] W. J. Percival and M. White, Testing cosmological structure formation using redshift-space distortions, Mon. Not. R. Astron. Soc. **393,** 297 (2009).

[156] O. F. Hernández, Neutrino masses, scale-dependent growth, and redshift-space distortions, J. Cosmol. Astropart. Phys. 06 (2017) 018.

[157] F. Villaescusa-Navarro, A. Banerjee, N. Dalal, E. Castorina, R. Scoccimarro, R. Angulo, and D. N. Spergel, The imprint of neutrinos on clustering in redshift-space, Astrophys. J. **861,** 53 (2018).

[158] F. Marulli, C. Carbone, M. Viel, L. Moscardini, and A. Cimatti, Effects of massive neutrinos on the large-scale structure of the Universe, Mon. Not. R. Astron. Soc. **418,** 346 (2011).

[159] A. Boyle and E. Komatsu, Deconstructing the neutrino mass constraint from galaxy redshift surveys, J. Cosmol. Astropart. Phys. 03 (2018) 035.

[160] H. E. S. Velten, R. F. vom Marttens, and W. Zimdahl, Aspects of the cosmological "coincidence problem", Eur. Phys. J. C **74,** 3160 (2014).

[161] J. Muir *et al.* (DES Collaboration), DES Y1 results: Splitting growth and geometry to test ΛCDM, arXiv:2010.05924.

[162] N. S. Kern, A. Liu, A. R. Parsons, A. Mesinger, and B. Greig, Emulating simulations of cosmic dawn for 21 cm power spectrum constraints on cosmology, reionization, and x-ray heating, Astrophys. J. **848,** 23 (2017).

[163] O. Lahav, A. Kiakotou, F. B. Abdalla, and C. Blake, Forecasting neutrino masses from galaxy clustering in the dark energy survey combined with the Planck measurements, Mon. Not. R. Astron. Soc. **405,** 168 (2010).

[164] T. Brinckmann, D. C. Hooper, M. Archidiacono, J. Lesgourgues, and T. Sprenger, The promising future of a robust cosmological neutrino mass measurement, J. Cosmol. Astropart. Phys. 01 (2019) 059.

[165] A. Boyle, C. Uhlemann, O. Friedrich, A. Barthelemy, S. Codis, F. Bernardeau, C. Giocoli, and M. Baldi, Nuw CDM cosmology from the weak lensing convergence PDF, Mon. Not. R. Astron. Soc. **505,** 2886 (2021).

[166] R. Pearson and O. Zahn, Cosmology from cross correlation of CMB lensing and galaxy surveys, Phys. Rev. D **89,** 043516 (2014).

[167] E. Giusarma, S. Vagnozzi, S. Ho, S. Ferraro, K. Freese, R. Kamen-Rubio, and K.-B. Luk, Scale-dependent galaxy bias, CMB lensing-galaxy cross-correlation, and neutrino masses, Phys. Rev. D **98,** 123526 (2018).

[168] B. Yu, R. Z. Knight, B. D. Sherwin, S. Ferraro, L. Knox, and M. Schmittfull, Towards neutrino mass from cosmology without optical depth information, arXiv:1809.02120.

[169] L. Xu, Probing the neutrino mass through the cross correlation between the Rees-Sciama effect and weak lensing, J. Cosmol. Astropart. Phys. 08 (2016) 059.

[170] A. E. Bayer, F. Villaescusa-Navarro, E. Massara, J. Liu, D. N. Spergel, L. Verde, B. Wandelt, M. Viel, and S. Ho, Detecting neutrino mass by combining matter clustering, halos, and voids, Astrophys. J. **919,** 24 (2021).

[171] S. Saito, M. Takada, and A. Taruya, Impact of Massive Neutrinos on the Nonlinear Matter Power Spectrum, Phys. Rev. Lett. **100,** 191301 (2008).

[172] J. Brandbyge and S. Hannestad, Resolving cosmic neutrino structure: A hybrid neutrinoN-body scheme, J. Cosmol. Astropart. Phys. 01 2010, 021 (2010).

[173] J. Lesgourgues, S. Matarrese, M. Pietroni, and A. Riotto, Non-linear power spectrum including massive neutrinos: The time-RG flow approach, J. Cosmol. Astropart. Phys. 06 (2009) 017.

[174] Y. Y. Y. Wong, Neutrino mass in cosmology: Status and prospects, Annu. Rev. Nucl. Part. Sci. **61,** 69 (2011).

[175] S. Bird, M. Viel, and M. G. Haehnelt, Massive neutrinos and the non-linear matter power spectrum, Mon. Not. R. Astron. Soc. **420,** 2551 (2012).

[176] J. Adamek, R. Durrer, and M. Kunz, Relativistic N-body simulations with massive neutrinos, J. Cosmol. Astropart. Phys. 11 (2017) 004.

[177] F. Villaescusa-Navarro *et al.*, The quijote simulations, Astrophys. J. Suppl. Ser. **250,** 2 (2020).

[178] A. Mead, S. Brieden, T. Tröster, and C. Heymans, HMcode-2020: Improved modelling of non-linear cosmological power spectra with baryonic feedback, Mon. Not. R. Astron. Soc. **502,** 1401 (2021).

[179] C. B. de Senna Nascimento and M. LoverdeNeutrinos in N-body simulations, Phys. Rev. D **104,** 043512 (2021).

[180] B. Bose, B. S. Wright, M. Cataneo, A. Pourtsidou, C. Giocoli, L. Lombriser, I. G. McCarthy, M. Baldi, S. Pfeifer, and Q. Xia, On the road to percent accuracy V: The non-linear power spectrum beyond ΛCDM with massive neutrinos and baryonic feedback, Mon. Not. R. Astron. Soc. **508,** 2479 (2021).

[181] E. Castorina, C. Carbone, J. Bel, E. Sefusatti, and K. Dolag, DEMNUni: The clustering of large-scale structures in the presence of massive neutrinos, J. Cosmol. Astropart. Phys. 07 (2015) 043.

[182] A. Raccanelli, L. Verde, and F. Villaescusa-Navarro, Biases from neutrino bias: To worry or not to worry?, Mon. Not. R. Astron. Soc. **483,** 734 (2019).

[183] S. Vagnozzi, T. Brinckmann, M. Archidiacono, K. Freese, M. Gerbino, J. Lesgourgues, and T. Sprenger, Bias due to neutrinos must not uncorrect'd go, J. Cosmol. Astropart. Phys. 09 (2018) 001.

[184] C.-T. Chiang, M. LoVerde, and F. Villaescusa-Navarro, First Detection of Scale-Dependent Linear Halo Bias in *N*-Body Simulations with Massive Neutrinos, Phys. Rev. Lett. **122,** 041302 (2019).